CHAPTER 4
THEORY AND LAWS IMPLEMENTED IN TRIMON[1]

by M. R. Omar

In the previous chapters, most of the neutron transport theorems have been presented in detail, and these theorems will become the foundation of the development of a multigroup Monte Carlo code for TRIGA reactors. This chapter outlines the details of the development of TRIMON (**TRI**GA **Mon**te Carlo Code), a next-generation reactor code that integrates diffusion-theory-type group cross sections into the Monte Carlo method for TRIGA reactors. Also, this hybrid combination speeds up stochastic simulations via homogenization of complex local core regions. TRIGA reactors are currently installed in 24 different countries, therefore, a robust core management code must be written for their safety analysis. Also, TRIMON is written in Fortran90 programming language. In fact, Fortran90 is chosen due to its simple and elegant modular programming paradigm that enables the developers and users to emphasize on the theoretical implementation of the code without the need of advanced programming knowledge. TRIMON incorporates critical features that improve certain functionalities that are less optimal in most state-of-the-art Monte Carlo codes such as direct integration of local fuel burnup in core calculation, sophisticated reactor core design considerations and simulation time improvements in complex core configurations. TRIMON also excludes the intricate jargon related to the core geometry and tally specifications required by most general multi-purpose Monte Carlo codes during the process of translating TRIGA core problems.

---

[1] This chapter is adapted from the following published research article: Omar, M. R., Karim, J. A., & Yoon, T. L. (2019). *The development of a multigroup Monte Carlo code for TRIGA reactors.* Nuclear Engineering and Design, 342.

4.1 Introduction to TRIGA Reactors

TRIGA is a commercial research reactor built by General Atomics, USA. Now, the reactor has been installed in 24 different countries. The reactor has been used for many diverse applications such as radioisotopes production, non-destructive testing, research on the properties of matter and for education and training. The reactor is a pool-typed water reactor and the reactor core is loaded with hydride fuel-moderator element, specifically U-ZrH. Most neutron moderations take place in the fuel element itself and the neutron moderation is mainly due to H in H-Zr (Henry, Tiselj, & Snoj, 2017). The reactor utilises demineralized water as coolant and moderator, where the loaded fuels are cooled by the flow of the coolant through the reactor core through natural convection or by forced cooling which depends on the reactor design.

TRIGA reactors are well recognised for its built-in safety characteristic due to a physical property of U-ZrH fuel. Here, TRIGA reactors have large prompt negative temperature coefficient. This implies that it is adequate to control an unexpected large insertion of positive reactivity to the reactor core. The fuel meat is a solid, homogeneous alloy of U-ZrH with the uranium enriched to 20% U-235. Also, the fuel meat is clad by a 0.051cm thick aluminium or stainless steel (SUS304) can.

Reaktor TRIGA Puspati (RTP) is a 1 MWth research reactor that has been installed in 1982 at Malaysian Nuclear Agency, Bangi, Malaysia. RTP core is a cylindrical-shaped core holding 127 designated core locations to accommodate fuel elements and other non-fuel elements such as control rods and irradiation facilities. The reactor core and the reflector assembly are mounted at the bottom of an aluminium tank situated inside the concrete shielding. The reactor core and experimental facilities are enclosed by a high-density concrete shielding. The reflector is made up of graphite and the reactor assembly is equipped with four boron carbide control rods. To provide vertical shielding, water is filled about 5m above the reactor core. Each element is arranged in seven concentric rings designated as Ring-A, Ring-B, …, Ring-G with 1, 6, 12, 18, 24, 30 and 36 core locations respectively.

4.2 TRIGA Core Unit Cells and Core Meshing

Theoretically, a reactor core can be built using its primary lattice structures which are identified as unit cells. The geometry of the unit cells is specified such that the complete reactor core can be formed using copies of these unit cells. For example, the unit cells forming a TRIGA core are illustrated in Fig. 4.1. A heterogeneous unit cell is composed of some separated regions of materials. In contrast, a homogenized unit cell is assigned such that the separated regions are “blended” while maintaining the integral neutron behaviour. In this context, neutron behaviour is a series of events where numerous neutron-nucleus interactions take place.

Essentially, a homogenized macroscopic neutron cross section, $\overline{\Sigma}$, is defined such that when they are used in the calculation of a homogenized unit cell, the net neutron leakage, the total neutron absorption and the total reaction rate remain the same as obtained in the calculation of the heterogeneous unit cell (International Atomic Energy Agency (IAEA), 1980). In TRIMON, each unit cell represents a homogenized reactor sub-region with constant neutron cross section. Customarily, when tracing the

random walks of a neutron history, the current unit cell which holds the neutron is mapped so that the value of $\overline{\Sigma}$ for the cell can be retrieved and used for simulating the succeeding nuclear events.

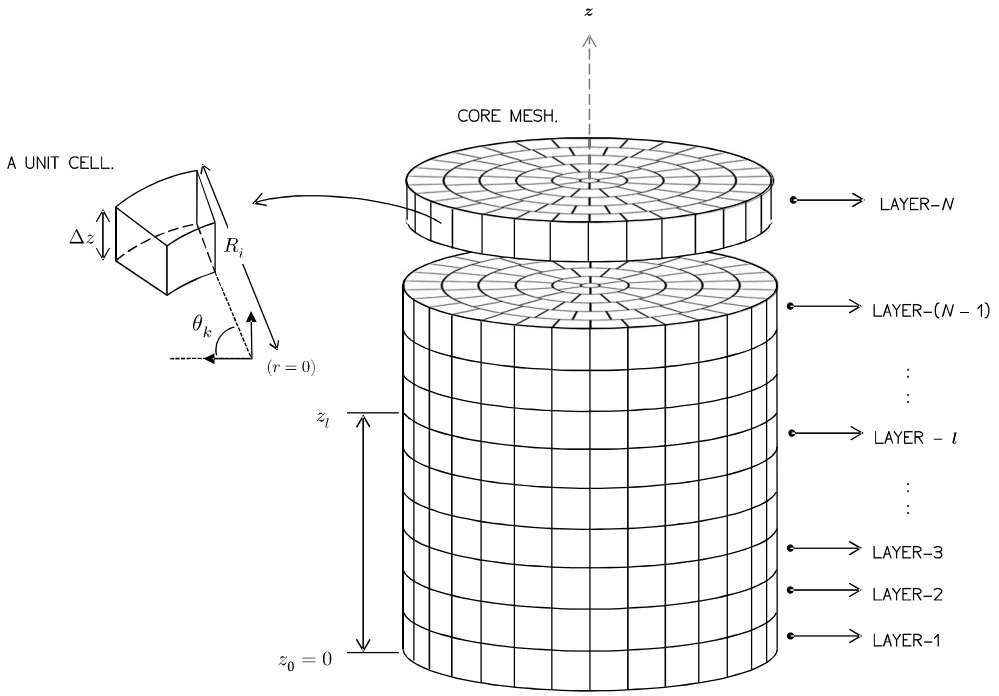

Figure 4.1: An assembly of unit cells forming a TRIGA reactor core.

To apply a similar concept to a TRIGA core, a unit cell is identified using cell indices $\langle i, k, l \rangle$. The radial position of the unit cell, R_i is determined using the radial index, i. The angular bearing of the unit cell, $\theta_{i,k}$ can be determined using combinations of the radial index and the angular index, $\langle i, k \rangle$. The cylindrical reactor core is sliced into several layers of equal thickness, Δz. Dividing the core into several layers will identify the z-axis position of the unit cell, z_l. A core layer can be determined using the core layer index, l. The position, $\mathbf{P}$, of a unit cell in the cylindrical coordinate system can be mapped using the set of cell indices $\langle i, k, l \rangle$. The relationship is defined as,

$$\mathbf{P} = R_i \, \mathbf{e}_{\boldsymbol{r}} + \frac{\pi}{6} \frac{2k-1}{i-1} \mathbf{e}_{\boldsymbol{\theta}} + l \Delta z \, \mathbf{e}_{\boldsymbol{z}}, \tag{4.1}$$

where $\mathrm{e}_{\boldsymbol{r}}$, $\mathrm{e}_{\boldsymbol{\theta}}$ and $\mathrm{e}_{\boldsymbol{z}}$ are the basis vectors that define the cylindrical coordinates. A more comprehensive details of a TRIGA core meshing structure implemented in TRIMON is given in *Appendix B*.

4.3 Cell Homogenization

In common, the homogenization method starts with the transport calculation at the heterogeneous unit cell level. Subsequently, a heterogeneous unit cell is represented

using its equivalent homogeneous unit cell of equal volume. Normally, a unit cell that includes fuel materials is assigned as a fuel cell. In a typical TRIGA core, a single fuel cell comprises a set of fuel regions plus the surrounding coolant water gap. A Zr rod is positioned at the centre of the fuel element (see Fig. 4.2). In TRIMON, only the active part of the fuel element is considered since it is the central part that drives the reactor core power generation.

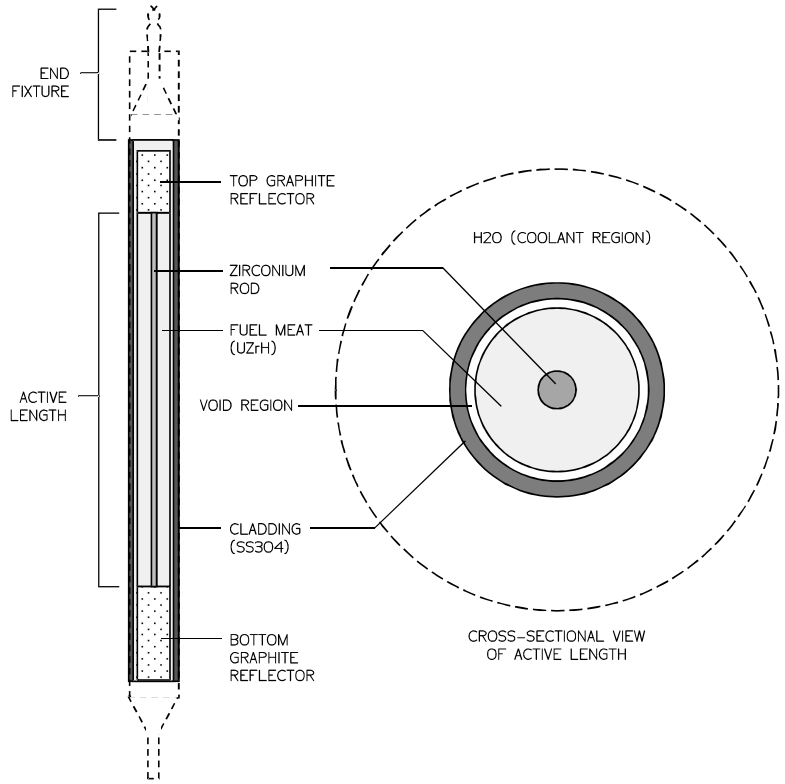

Figure 4.2: A schematic diagram of a TRIGA standard fuel element.

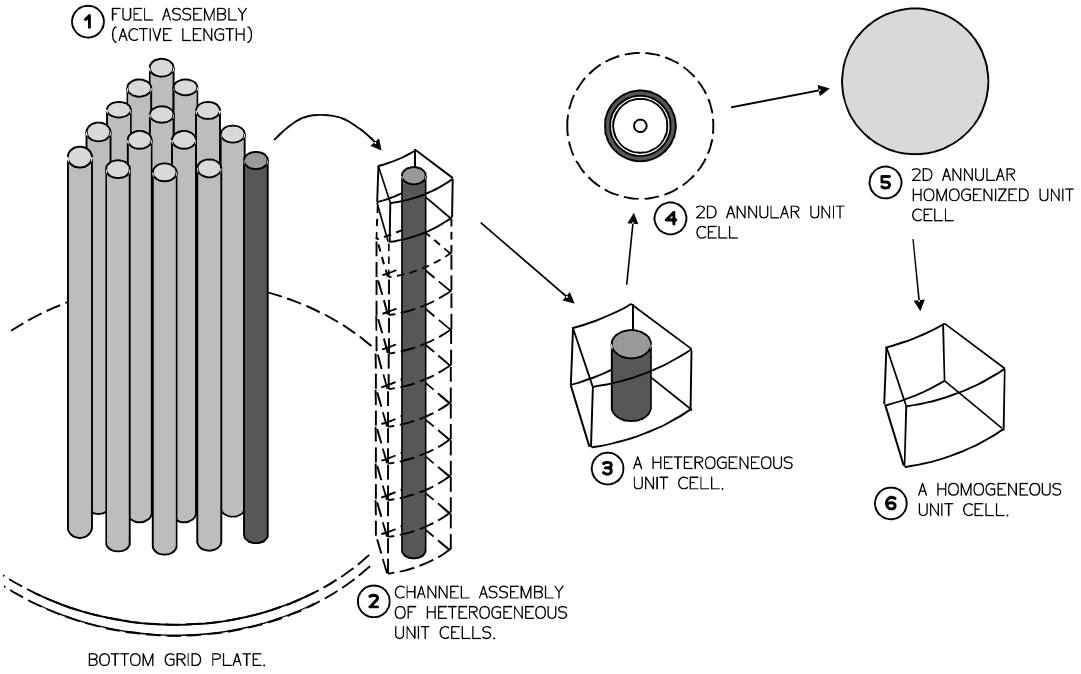

Figure 4.3: An overview of the steps involved in the procedure of homogenizing a unit cell.

Examine the illustration of a TRIGA core shown in Fig. 4.3. Suppose that a heterogeneous unit cell is taken from the core. For an annular TRIGA reactor core, one can effectively substitute a heterogeneous unit cell with a similar heterogeneous annular cell of equal volume. Following, the annular unit cell is accurately modelled in two-dimensional geometry to approximate the heterogeneous unit cell. At this level, the transport calculation of the two-dimensional model is performed to get the reference flux spectrum for the next homogenization step.

Neutrons will experience isotropic scattering as they arrive the cell boundary of the two-dimensional model (Trkov & Ravnik, 1994). Therefore, the transport problem at the unit cell level is indistinguishable to one involving a huge reactor core which is formed by many identical unit cells. Besides, the heterogeneous modelling method intends to achieve the best estimate of the original reactor core.

Next, the homogenization method continues with the use of the Effective Diffusion Homogenization (EDH) method (Trkov & Ravnik, 1994) for obtaining the homogenized neutron cross sections. Essentially, EDH method gives the approximate treatment of the radial leakage of the unit cell. Aside from maintaining the total reaction rates, the radial leakage in both homogeneous and heterogeneous unit cells is also conserved. So, this helps to decouple transport calculations of the unit cell from its surroundings. In essence, TRIMON employs the homogenization steps outlined by (Trkov & Ravnik, 1994).

Finally, a set of homogenized group neutron cross sections is obtained from the unit cell. The unit cell homogenization method is repeated for all unit cells within the reactor core. The calculated homogenized group neutron cross sections are grouped and compiled into a TRIGA cross section file (*.txs* file) and serve as a lookup table of

the homogenized cross sections for the next full core Monte Carlo simulation. The details of the contents of a *.txs* file is given in *Appendix C*.

4.4 Fuel Burnup Effect

In TRIMON, fuel burnup accumulation due to previous core operations is not ignored during cross section data pre-processing. Fuel depletion correction of neutron cross sections implemented in TRIMON does not need any additional fuel depletion codes as existing fuel depletion empirical relations are used. Fuel depletion calculation in TRIMON is based on the pre-defined correlations of the remaining mass fraction of U-235 in per cent, b, and its equivalent fuel burnup in MWd. Also, each predefined correlation is defined for a specific TRIGA fuel type, i.e. standard U-ZrH fuel types such as FE08 for 8.5%wt U, FE12 for 12%wt U and FE20 for 20%wt U.

In TRIMON, a fuel element is equally sliced axially into several fuel unit cells, where each unit cell holds a specific burnup level, b. The burnup, b, for each fuel unit cell in per cent U-235 is given by the general power series correlation,

$$b = \sum_{j=1}^{N} \beta_j p_{\text{cell}}^{j} (\Delta t)^j \tag{4.2}$$

where N is the order of the series, β_j are the coefficients of the series, p_{cell} is the fission power deposited in the cell, and Δt is the burnup increment in days. In TRIMON, the pre-set values of β_j were determined based on the WIMS calculations done by (A. Persic, Slavic, Ravnik, & Zagar, 1998) and the results of the calculation for each different standard U-ZrH fuel types are shown in Fig. 4.4. Plus, each type of fuel is assigned to a specific set of β_j. It is important to note that the values of β_j can be prescribed by the user through the main code input file. During each cell calculation, the fuel density and enrichment are corrected according to the prescribed value of b so that the number density of the fuel region within the cell can re-calculated.

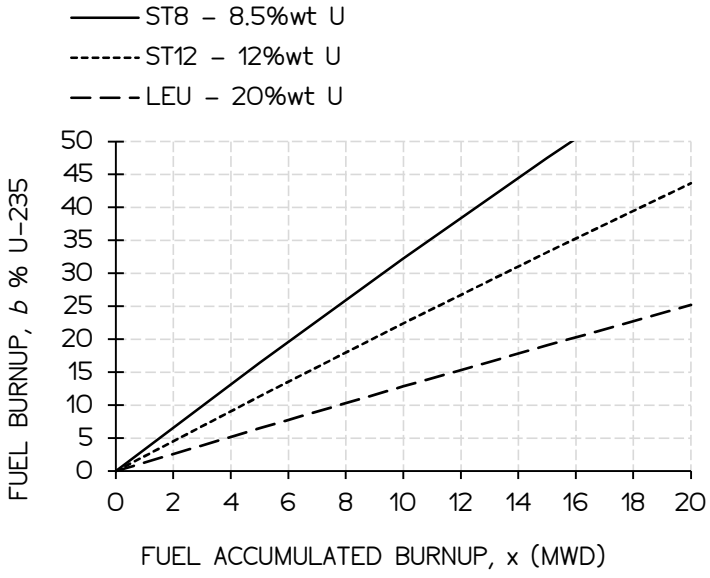

Figure 4.4: Fuel burnup in % U-235 correlations for different standard U-ZrH fuel types, 8.5%wt (ST8), 12%wt (ST12) and 20%wt (LEU). (A. Persic et al., 1998)

4.5 Fuel Temperature Effect

There is a clear correlation between the average fuel burnup and fuel temperature because the total fission energy liberated by the fuel material is largely exchanged into thermal energy. Inescapably, fuel temperature instigates the Doppler broadening of the neutron cross section's resonance region (Carter & Cashwell, 1975), therefore it greatly affects the heterogeneous cell's flux spectrum for the purpose of homogenization calculation. Principally, the temperature of a fuel cell is dependent on its position inside the core. For a TRIGA reactor, the temperature of a fuel cell is stemmed based on the empirical formula recommended by (Peršič et al., 2017),

$$T_{\text{cell}} = T_{\text{cool}} + \sum_{n=1}^{N} a_n \alpha_r \alpha_z \left\{ \frac{m}{M} \left(1 - \frac{b}{100} \right) P \right\}^n \tag{4.3}$$

where:

T_{cool} is the temperature of the coolant,

N is the power series order,

a_n is the coefficient of the power series,

α_r is the radial power form factor in the fuel cell location,

α_z is the axial power form factor at the fuel cell location,

m is the mass of Uranium in the fuel rod,

M is the total mass of Uranium within the reactor core,

b is the fuel rod burnup in per cent, and,

P is the nominal core power.

The fuel cladding temperature is provided by the average of T_{cool} and T_{cell}. The values of constants, a_n, are verified experimentally and needs to be indicated by the user in the code input. In TRIMON, Eq. (4.3) can be expressed as a piecewise function, such that a different set of a_n is designated to a different cell power interval.

4.6 Power Form Factors

The power form factor, α, of a reactor core portrays the profile of the power distribution inside a reactor core. In fact, it regulates the fuel temperature distribution relative to the hottest spot within a reactor core. Bear in mind that fuel temperature Doppler broadens a neutron cross section's resonance region, thus, α is a notable tool for scrutinizing the accuracy of the core simulation results. In the extent of this work,

there are two types of power form factor to be pondered – the radial power form factor, α_r and the axial power form factor, α_z.

Meanwhile, TRIMON provides three-dimensional power distribution, the radial and axial power form factors can also be determined using TRIMON by the use of the algorithm summarized in Fig. 4.5. Notice also that power peaking factors can be calculated according to the straightforward method outlined by (Snoj & Ravnik, 2008).

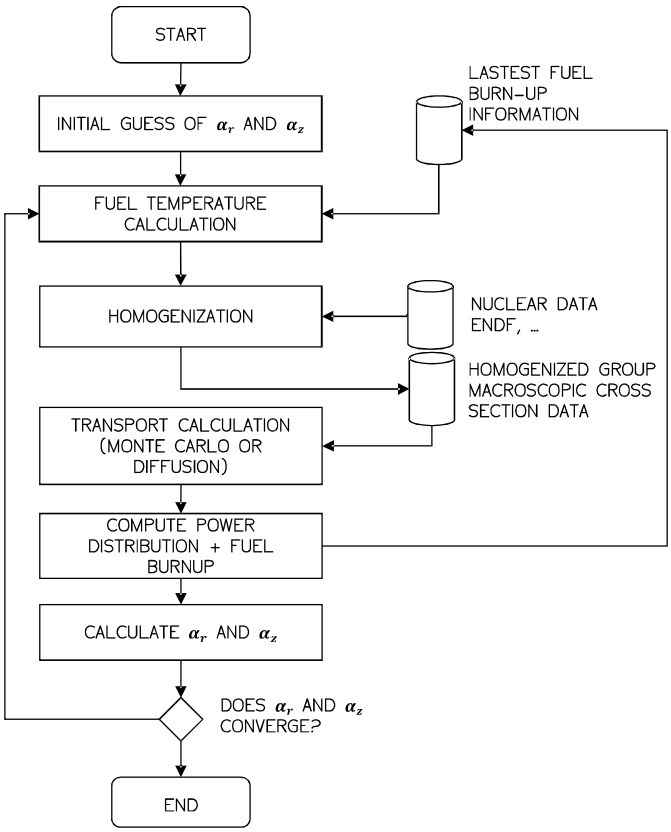

Figure 4.5: Simplified steps involved in the calculation of power peaking factors in TRIMON.

4.7 Homogenized Multigroup Monte Carlo Method

The Monte Carlo method is a technique of unravelling a deterministic problem by a stochastic approach by the use of neutron random walks. A number M of independent observations (e.g. neutron histories) are accumulated and the result is obtained from the averaged observation. The Monte Carlo method is frequently applied to deterministic problems that are hard to solve by deterministic methods. The main benefits of the Monte Carlo method include its straightforwardness where the transport equation does not have to be formulated to obtain the neutron flux in the reactor. And also, it applies to complicated problems without simplifications, for instance, it can model an exact complicated nuclear reactor core geometry.

In the Monte Carlo method, each neutron is simulated from the birth of a neutron until the death event of the neutron (i.e. due to a disappearance reaction or leakage). However, the Monte Carlo method presented in this work is distinctive from the usual method, where homogenized group neutron cross-section data is employed to enhance

the simulation efficiency. In the conventional Monte Carlo method, non-homogenized neutron cross section data are used, which in fact increasing the complexity of the simulation. According to the homogenization theory discussed in Chapter 3, a non-homogenized or heterogeneous region may comprise of many different types of materials with different cross section values. Thus, in the conventional method, more stochastic calculations need to be accomplished to accommodate all of the different types of materials. However, a homogenized region comprised of a single pseudo-material with a single group neutron cross section will effectively reduce the number of stochastic calculations compared with the conventional Monte Carlo method.

4.7.1 Overview of Monte Carlo Method Implemented in TRIMON

In TRIMON, neutrons are anticipated to be travelling in a straight line in the direction $\widehat{\mathbf{\Omega}} = (u, v, w)$ from an initial position, $\mathbf{r}_0$. Also, it assumes that the neutron is only generated by a fission reaction. Other types of neutron production are disregarded, and their effects are insignificant. For occasion, nearly all (n, xn) reactions happen at high incident neutron energy, normally beyond 10MeV. Consequently, such a reaction is atypical since a huge fraction of neutrons in a thermal reactor holds an energy regime of less than 10MeV. Neutron production reaction caused by other sorts of particles is also abandoned since these particles are not tracked.

As a general rule, when a neutron journeys within a homogenized unit cell, there is a likelihood that it will strike a nucleus of the homogenized unit cell material. Throughout this collision, there are only three types of reactions counted – neutron absorption, neutron elastic scattering and fission reaction. It is sensible to bring to mind that the Monte Carlo method designated in this research utilizes homogenized neutron cross sections. Then, it is crucial to highlight that all neutron behaviours within the homogenized unit cell are virtual.

Nevertheless, when these virtual behaviours are integrated over the whole volume of the unit cell, they bear a resemblance to the overall behaviour of the neutrons when the heterogeneous neutron cross sections are used in the simulation. Astonishingly, a similar idea is spotted in the delta tracking method in Monte Carlo explained by (Leppänen, 2010). In delta tracking method, the concept of virtual collision is employed, and it effectively homogenized the material total cross section in a way that the total neutron path length within a whole geometry is conserved.

4.7.2 Distance to Next Collision and Random Walks

As a rule, a neutron is set off at a position $\mathbf{r}_0$ and stops at the point of the next collision event, $\mathbf{r}_c$. Afterwards, the current unit cell, $\langle i, k, l \rangle$, is mapped where the position $\mathbf{r}_0$ is embedded inside $\langle i, k, l \rangle$. Consequently, the distance to the next collision, $\|\mathbf{r}_c - \mathbf{r}_0\|$, can be calculated,

$$\|\mathbf{r}_c - \mathbf{r}_0\| = -\frac{\ln \zeta}{\bar{\Sigma}_{t,ikl}} \tag{4.4}$$

where $\overline{\Sigma}_{\mathrm{t},ikl}$ is the total homogenized neutron cross section of the unit cell $\langle i,k,l\rangle$ and ζ is a random number where $\zeta \in [0,1)$.

Trailing the transport process further, the distance to the nearest boundary of the current unit cell, $\|\mathbf{r}_b - \mathbf{r}_0\|$, along the neutron trajectory direction, $\widehat{\mathbf{\Omega}}$, is calculated. If the distance to the next collision event is larger than the distance to the nearest cell boundary, i.e., $\|\mathbf{r}_c - \mathbf{r}_0\| > \|\mathbf{r}_b - \mathbf{r}_0\|$, subsequently, the neutron is transported to the nearest boundary. Or else, the neutron is transported to the next collision location, $\mathbf{r}_c$. To sum up, the final location of the neutron is given by,

$$\mathbf{r} = \mathbf{r}_0 + \min(\|\mathbf{r}_c - \mathbf{r}_0\|, \|\mathbf{r}_b - \mathbf{r}_0\|)\,\widehat{\mathbf{\Omega}} \tag{4.5}$$

At the collision site, the neutron will progress for a neutron–nuclear interaction. Contrariwise, if the neutron is transported to the cell boundary, the distance to the next collision will be calculated using the total neutron cross section of the neighbouring unit cell. This process repeats until the neutron is absorbed by a nucleus or leak out of the reactor core. As soon as the neutron is absorbed, the simulation ends and the next neutron from the fission source bank is simulated.

4.7.3 Distance to the Nearest Cell Boundary

At first, a set of boundary surfaces, β, that characterize the boundary of a homogeneous unit cell is taken into consideration. Easily, the distance of a neutron to each boundary surface $b \in \beta$ along the neutron flight direction $\widehat{\mathbf{\Omega}}$ is given by $\|\mathbf{r}_b - \mathbf{r}_0\|$. Consider a neutron at $\mathbf{r}_0$ is moving in the direction $\widehat{\mathbf{\Omega}}$. To calculate $\|\mathbf{r}_b - \mathbf{r}_0\|$, one must solve the surface equation of the boundary of the unit cell,

$$f_s\left(\mathbf{r}_0 + \|\mathbf{r}_b - \mathbf{r}_0\|\widehat{\mathbf{\Omega}}\right) = 0 \tag{4.6}$$

where $f_s(\mathbf{r})$ is the surface equation of b.

It is essential to mention that the solution to Eq. (4.6) can be more than one and can be real or complex. Undoubtedly, if the solutions are all complex, therefore the direction of flight will never cross with the surface. Then again, a real solution which is less than zero implies that the surface is behind the neutron flight path. Preferably, a positive real solution is always chosen. To finish, the minimum of the positive solutions is selected to be the value of $\|\mathbf{r}_b - \mathbf{r}_0\|$. In addition, a detailed calculation of the distance to each surface of a TRIGA core unit cell is given in *Appendix D* for readers reference.

4.7.4 Sampling a Reaction at the Collision Site

TRIMON distinguishes three major neutron-nucleus interactions – neutron capture, neutron elastic scattering and fission. In addition, neutron absorption includes entirely other types of reaction such as (n, p), (n, α), etc. Moreover, all of these reactions involve capturing a neutron to give off secondary particles except neutrons. Focusing on fission reaction, it is regarded as an absorption reaction because a nucleus absorbs a neutron before dividing into two daughter nuclei in the course of fission event.

In effect, the homogenized material is supposed to contain a single type of nucleus with a set of homogenized group cross sections that is constant throughout the unit cell. Consequently, one does not need to sample any nuclide of collision. First of all, the total macroscopic cross section of the unit cell is retrieved from the homogenized group neutron cross section data. In the second place, if a neutron in energy group g experiences collision with a nucleus within a unit cell, the first step is to decide whether the neutron is absorbed by the nucleus. To finish, this procedure is based on the algorithm outlined by (Romano & Forget, 2013),

1. A random number, ζ, is obtained from the random number generator.
2. The neutron is killed if the following condition is met,

$$\zeta < \frac{\overline{\Sigma}_{\mathrm{a}}^{g} - \overline{\Sigma}_{\mathrm{f}}^{g}}{\overline{\Sigma}_{\mathrm{t}}(g)} \tag{4.7}$$

where $\overline{\Sigma}_{\mathrm{a}}^{g}$ is the homogenized absorption cross section, $\overline{\Sigma}_{\mathrm{f}}^{g}$ is the homogenized fission cross section and $\overline{\Sigma}_{\mathrm{t}}^{g}$ is the homogenized total macroscopic cross section the unit cell. Finally, the neutron history tracking is terminated and the next neutron in the fission bank is simulated.

4.7.5 Multi-Group Scattering

Basically, the neutron energy and direction are transformed after a neutron scattering event. Therefore, the outgoing energy group g' and the outgoing direction $\hat{\boldsymbol{\Omega}}'$ of the neutron following a scattering event is calculated. If a homogeneous group cross section data employs G neutron groups, thus the group scattering cross section from the incident energy group g to all existing outgoing energy groups are queried from the homogenized cross section data table.

At the initial stage of processing a group scattering event, a random number $\zeta \in [0,1)$ is selected from the random number generator. Then, the outgoing energy group of the neutron is chosen using the inverse sampling method, such that the value of ζ is compared to the cumulative distribution function, $F(g \to g')$, of the outgoing energy group, g', for the given incoming energy group, g. The cumulative distribution function can be stated as,

$$F_g(g \to g') = \sum_{1 \le \gamma \le g'} \frac{\overline{\Sigma}_{\mathrm{s}}^{g \to \gamma}}{\overline{\Sigma}_{\mathrm{t}}^{g} - \overline{\Sigma}_{\mathrm{a}}^{g}} \tag{4.8}$$

where $\overline{\Sigma}_{\mathrm{s}}$ is the homogenized scattering cross section, $\overline{\Sigma}_{\mathrm{t}}$ is the homogenized total neutron cross section and $\overline{\Sigma}_{\mathrm{a}}$ is the homogenized absorption cross section. Suitably, the term $\overline{\Sigma}_{\mathrm{t}} - \overline{\Sigma}_{\mathrm{a}}$ is the total homogenized scattering cross section, in any case of any outgoing energy group. A similar method can be done to pick out the outgoing angle of the neutron. Contrariwise, one can sample the value of μ by making use of the following relation if the scattering direction is expected to be isotropic,

$$\mu = 2\zeta - 1. \tag{4.9}$$

Automatically, the outgoing neutron direction can be calculated given that the outgoing energy and scattering cosine have been determined. The scattering cosine μ denotes the cosine of the angle between incident neutron direction, $\hat{\mathbf{\Omega}}$, and the outgoing neutron direction $\hat{\mathbf{\Omega}}'$. The scattering cosine is expressed as,

$$\mu = \hat{\mathbf{\Omega}}' \cdot \hat{\mathbf{\Omega}} \tag{4.10}$$

Accordingly, it is probable to determine $\hat{\mathbf{\Omega}}'$ by sampling an azimuthal angle $\phi \in [0,2\pi)$ from the uniform distribution. If the components of $\hat{\mathbf{\Omega}}'$ and $\hat{\mathbf{\Omega}}$ are given as (u', v', w') and (u, v, w) respectively, the relationship between $\hat{\mathbf{\Omega}}'$ and $\hat{\mathbf{\Omega}}$ is given by (Romano & Forget, 2013),

$$u' = \mu u + \sqrt{\frac{1-\mu^2}{1-w^2}}(uw\cos\phi - v\sin\phi) \tag{4.11}$$

$$v' = \mu v + \sqrt{\frac{1-\mu^2}{1-w^2}}(vw\cos\phi - u\sin\phi) \tag{4.12}$$

$$w' = \mu w + \sqrt{1-\mu^2}\sqrt{1-w^2}\cos\phi \tag{4.13}$$

4.7.6 Fission Reaction

Despite the fact that fission is considered as an absorption reaction (A. Persic et al., 1998), TRIMON deals with fission similarly to inelastic scattering. This is because fission neutrons are set off as the outcome of the fission event. At the early step of a fission process, the average number of fission neutrons, ν_g, is estimated based on the incoming neutron energy group, g. In particular, the correlation relation between υ_g and g is given by (A. Persic et al., 1998)

$$\nu_g = 2.55 - 0.11\frac{g-1}{\max(1, G-1)} \tag{4.14}$$

where G is the total number of energy groups used in the simulation. After that, the total number of neutrons to be emanated after the fission event, ν, is predicted using the method summarized by (Romano & Forget, 2013). Then again, homogenized cross sections are used instead. The value of ν can be determined using,

$$\nu = \frac{W\nu_g\overline{\Sigma}_{\mathrm{f}}}{k_{n-1}\overline{\Sigma}_{\mathrm{t}}} \tag{4.15}$$

where W is the neutron weight and k_{n-1} is the value of k_{eff} from the previous fission cycle. Here, the value of ν is rounded to the nearest integer.

Later, the outgoing energy of these fission neutrons is sampled. It is appropriate to make known to the cumulative fission energy group spectrum, $F(g')$, which is defined as the cumulative probability of having energy group g' as the outgoing fission

neutron energy group. In most cases, one can sample the outgoing energy of a fission neutron from Watt Distribution. In summary, $F(g')$ is expressed as,

$$F(g') = \sum_{\gamma \leq g'} \int_{\gamma} \mathrm{d}E' c\ \mathrm{e}^{-aE'} \sinh\ \sqrt{bE'} \tag{4.16}$$

where $c = 0.453$, $a = 1.036$, $b = 2.29$ (Duderstadt & Hamilton, 1976) and E' is the outgoing energy variable. Notice that the integration limits are the energy boundaries that define the entire outgoing energy group γ. Consequently, a random number, ζ is obtained from the random number generator and the outgoing energy group is determined using the inverse sampling method (Ross & Ross, 2013) where the value of ζ is compared to $F(g')$ and the corresponding value of g' is determined.

The finishing step is to sample the outgoing direction, $\hat{\mathbf{\Omega}}'$, of the fission neutron. In TRIMON, the outgoing angle of a fission neutron is isotropic at all instances. Certainly, the algorithm used to sample the outgoing direction of a neutron after isotropic scattering is used for predicting the outgoing direction of a fission neutron.

4.7.7 Cell Flux Tally Scoring and Calculation of Fuel Element Power

TRIMON make use of track length estimators when collecting flux tallies of an entire volume of a unit cell. Nevertheless, tallies collection is not done for a volume lesser than the volume of the unit cell due to unit cell homogenization. Actually, all collisions that occur inside a homogenized unit cell are virtual, thus, tallies accumulation for a volume smaller than the unit cell is improper.

According to (Romano & Forget, 2013), the derivation of track length flux estimator begins with the volume integrated flux for a specific neutron energy group,

$$V_{\text{cell}}\ \phi_g = \iiint \left[\int_{E_g}^{E_{g-1}} \psi(\mathbf{r}, \hat{\mathbf{\Omega}}, E, t)\ dE \right] d\mathbf{\Omega}\ dr\ dt \tag{4.17}$$

where ψ is the angular flux and V_{cell} is the volume of the unit cell of concern. Observe also that ψ can be rewritten in terms of the neutron density function, $N(\mathbf{r}, E, t)$, therefore,

$$V_{\text{cell}}\ \phi_g = \iint \left[\int_{E_g}^{E_{g-1}} \upsilon N(\mathbf{r}, E, t)\ dE \right] dr\ dt, \tag{4.18}$$

where υ is the average neutron speed. Using the basic classical mechanics' formula, $dt = dl/\upsilon$, yields,

$$V_{\text{cell}}\ \phi_g = \iint \left[\int_{E_g}^{E_{g-1}} N(\mathbf{r}, E, t)\ dE \right] dr\ dl\ . \tag{4.19}$$

From Eq. (4.19), the $\int dl$ term indicates that the total distance travelled by any neutrons in the entire cell must be calculated. The remaining terms indicate that the number of neutrons in energy group g at any position within the unit cell needs to be accumulated. Consequently, the track length estimator of the relative flux for neutron energy group g is given by,

$$\phi_g(i,k,l) = \frac{1}{W} \sum_{k \in \lambda} w_k(g) l_k, \tag{4.20}$$

where λ is the set of all tracks within the unit cell $\langle i,k,l \rangle$.

In the cylindrical coordinate system, the power radiated by a fuel element, P_{el}, is given as (A. Persic et al., 1998),

$$P_{\text{el}} = p_0 \iiint_{V_{\text{el}}} \phi(r,\theta,z)\, \overline{\Sigma}_{\text{f}}(r,\theta,z)\, dr\, d\theta\, dz, \tag{4.21}$$

where p_0 is the normalization factor, ϕ is the neutron flux and $\overline{\Sigma}_{\text{f}}$ is the homogenized fission cross section. The normalization factor can be calculated using,

$$p_0 = P \left[\iiint_{V_{\text{core}}} \phi(r,\theta,z)\, \overline{\Sigma}_{\text{f}}(r,\theta,z)\, dr\, d\theta\, dz \right]^{-1}. \tag{4.22}$$

Here, P is the nominal power of the reactor core in kW. Recall that a unit cell can be identified using the cell indices $\langle i,k,l \rangle$. A fuel element occupies the total volume of unit cells which have the same i and k values. Thus, the volume integral in Eqs. (4.21) and (4.22) can be numerically evaluated using,

$$P_{\text{el}} = p(i,k) = p_0 \sum_{l=1}^{n_l} \sum_{\forall g} \phi_g(i,k,l)\, \overline{\Sigma}_{\text{f}}^{g}(i,k,l), \tag{4.23}$$

where n_l is the total number of core layers, and

$$p_0 = P \left[\sum_{\forall (i,k,l)} \sum_{\forall g} \phi_g(i,k,l)\, \overline{\Sigma}_{\text{f}}^{g}(i,k,l) \right]^{-1}. \tag{4.24}$$

Note also that in Eq. (4.23), the summations include all neutron energy groups for all unit cells within the fuel element channel. On the other hand, the summations in Eq. (4.24) include all neutron energy groups for all unit cells within the reactor core.

4.8 Monte Carlo Criticality Calculation in TRIMON

In general, criticality calculation, or sometimes known as eigenvalue calculation is a transport simulation of neutrons studying the ability of a system, i.e. a nuclear reactor core, to sustain a fission chain reaction. In essence, TRIMON employs the Monte Carlo power iteration method to perform the criticality calculation of a TRIGA reactor. Recall that the Monte Carlo power iteration method necessitates history tracking of a finite number of neutrons from one generation to another. Conveniently, these generations are recognized as MC cycles. If fission happens during history tracking, the location of the fission site, the outgoing energy group and direction of the fission neutron and the weight of the neutron are kept for the use in the next MC cycle.

Since most Monte Carlo programmers represent neutron transport quantities using stacks, queues and arrays, the mathematical analysis incorporated in this book is expressed in terms of finite discrete phase space using vectors and matrices. The neutron phase space is discretized into cells, which is termed as phase space cells. To this point, any neutron that exits the problem phase space is considered escaped. Plus,

any functions of $\mathbf{r}$, $\hat{\mathbf{\Omega}}$ and E become vectors and any operators become square matrices. Most importantly, the order of all matrices and vectors is equal to the number of phase-space cells.

To begin with, it is convenient to define $\Phi^{(j)}$ as the expected number of neutrons in the corresponding phase-space cells during MC cycle j. Next, the eigen-equation in Eq. (3.63) can be further simplified into,

$$\begin{aligned}\Phi^{(j)} &= \frac{1}{k^{(j-1)}}(\mathbf{T}-\mathbf{S})^{-1}\mathbf{F}\Phi^{(j-1)} \\ &= \frac{1}{k^{(j-1)}}\mathbf{R}\Phi^{(j-1)}\end{aligned} \tag{4.25}$$

with $\mathbf{T}$, $\mathbf{S}$, $\mathbf{F}$ and $\mathbf{R}$ are square matrix operators with $\mathbf{R} \equiv (\mathbf{T}-\mathbf{S})^{-1}\mathbf{F}$, $k^{(j-1)}$ is the current estimate of the effective multiplication factor, and j is the iteration cycle index such that $j \geq 1$.

In this sense, the neutron source distribution of the current MC cycle, $\Phi^{(j)}$, can be determined by evaluating the matrix operation of the right-hand side of Eq. (4.25). Here, $\Phi^{(j-1)}$ is the neutron source distribution obtained from the previous MC cycle, $j-1$. In the Monte Carlo method, the right-hand side of Eq. (4.25) can be 'solved' by tracking neutrons that are selected from $\Phi^{(j-1)}$, starting from their birth location until their death after disappearance reactions. In this context, neutron disappearance reactions include fission and neutron capture by a nucleus.

To begin with, suppose M neutrons are randomly selected from $\Phi^{(j-1)}$ and initiated. Also, M is known as the neutron batch size. Each neutron is tracked from its starting point until its death due to escape, Russian roulette and so on. In addition, the total number of neutrons initiated during each MC cycle is always normalized to M. When simulating each of these neutrons, the collision site is determined, and the neutron is transported to the collision site. During each collision, m duplicates of the collision site are stored in $\Phi^{(j)}$ as the probable fission site and m is given by (X-5 Monte Carlo Team, 2005),

$$m = \frac{w}{k^{(j-1)}}\frac{\nu\Sigma_{\mathrm{f}}}{\Sigma_{\mathrm{t}}} + \zeta \tag{4.26}$$

where w is the particle weight of the neutron and ζ is a random number in [0, 1). Equally important, the value of $k^{(j)}$ can be estimated using the collision estimator where the $k^{(j)}$ estimator is accumulated during each collision i (X-5 Monte Carlo Team, 2005),

$$k_{\mathrm{col}}^{(j)} = \frac{1}{M}\sum_{i} w_i \nu \frac{\Sigma_{\mathrm{f}}}{\Sigma_{\mathrm{t}}}. \tag{4.27}$$

There are also other types of $k^{(j)}$ estimators, e.g. the absorption estimator and track-length estimator. However, the discussion of these estimators is beyond the scope of this paper. Finally, $\Phi^{(j)}$ is assigned as the fission neutron source for the next MC cycle.

The power iteration method is always prescribed with the initial guess of the neutron source distribution, $\Phi^{(0)}$. Briefly, as the iteration progresses from one MC cycle to another, $\Phi^{(j)}$ will stochastically converge to an equilibrium state which is also known as the stationary state. When stationarity is implied, tallies such as neutron flux, neutron lifetime and the effective multiplication factor can be accumulated, and their averages can be calculated at the end of the iterations.

It is important to ensure that the value of k_{eff} and the fission site distribution, $\Phi^{(j)}$, converge before any tally accumulation is made. In fact, $\Phi^{(j)}$ converges slower than that of k_{eff} (Cho & Chang, 2009). For k_{eff} the convergence can be observed from the plot of k_{eff} versus the number of fission cycles. The procedure outlined by (Romano & Forget, 2013) is applied to check whether $\Phi^{(j)}$ has converged, where the fraction of fission source sites that are present in each unit cell is calculated,

$$S_i = \frac{n_i}{n} \tag{4.28}$$

where n_i is the number of fission source sites in the i^{th} unit cell and n is the total number of fission source sites within the reactor core. Next, the Shannon entropy of Φ is calculated,

$$H_{\text{src}}\{\Phi\} = -\sum_{i=1}^{n} S_i \log_2 S_i \tag{4.29}$$

It is worthwhile to note that the convergence of H_{src} implies the convergence of Φ.

4.9 Code Design and Application

Principally, TRIMON is meant to simulate neutron transport problems in a TRIGA reactor core. Therefore, the material compositions of the reactor core are predefined in the code. And also, users do not need to identify the material compositions in the code input. The newly developed code recognizes core material compositions according to the core configuration, where each core channels are designated to various types of elements. A core channel may perhaps comprise of a fuel element or any various types of non-fuel element. The list of elements recognized by TRIMON is given in Table 4.1.

Principally, the TRIMON code comprises of two built-in modules. These modules are identified as WIMS Integrated TRIGA Cell Homogenization (WITCH) module and the Homogenized Group Monte Carlo (HGMC) module. WITCH module is intended to generate a homogenized neutron cross section lookup table (via a *.txs* file). Whereas the HGMC module is intended to perform the Monte Carlo simulation using the generated lookup table. It also produces the essential simulation outputs such as the power distribution, flux distribution and fuel burnups.

In relation with local fuel burnup consideration, the current accumulated burnup of fuel cells is acquired from the local burnup lookup table (the *zburn.out* file). Here, the lookup table is interpreted by WITCH module throughout the course of preparing the homogenized neutron cross section. Notice also that the local burnup table is updated after each burnup calculation.

Table 4.1: List of core channel elements.

Channel Element	Description
FE08, FE12, FE20	19.9% enriched $UZrH_{1.6}$ fuel element with 8.5%wt, 12%wt and 20%wt of uranium respectively; stainless steel (SS304) cladding. The fuel element is surrounded by coolant water.
CHN1	Irradiation Channel Type-I: An empty Al tube. CHN1 be used as an approximate model of a transient control rod.
CHN2	Irradiation Channel Type-II: Half void, half water in Al tube.
CHN3	Irradiation Channel Type-III: Full water in Al tube. Can be used to represent the central thimble of the reactor core.
GRAP	Graphite Element: Graphite in Al tube.
COOL	Coolant water (without Al tube)

The general workflow of TRIMON code is depicted in Fig. 4.6. TRIMON call for two input files to work. The case to be solved is given by the user through a formatted text file, *main.inp*, which contains various input cards. The second input file, *fuel_inventory.inp*, contains fuel elements information used in the calculation.

TRIMON code is set as a package which comprises of two different Windows™ program (*.exe*) files, where both programs execute WITCH and HGMC modules independently. These program files were created after the compilation of the source codes using the GNU Fortran compiler. The execution of these programs is not error-free since runtime errors may arise due to incorrect usage of input cards. Opportunely, the code is intended to alert users on particular error encounters through a comprehensible error message.

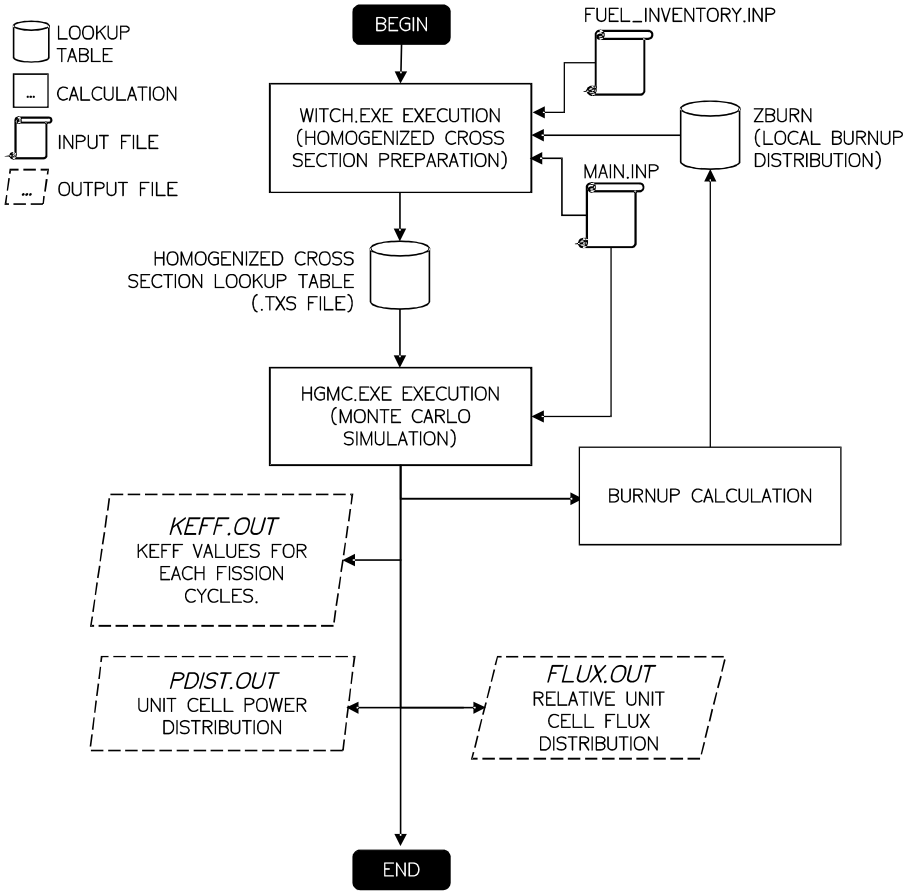

Figure 4.6: TRIMON code workflow.

4.10 TRIMON Validation and Benchmark Analysis

Unavoidably, it is compulsory for a newly developed neutron transport code to get validated in order to ensure its consistency in producing decent simulation results. At this point, TRIMON validation and tests were done in two ways. This includes comparing the code numerical output results with the actual operational reactor core data recorded in the reactor logbook and also by comparing the code simulation output results with the simulation output results produced by any well-established reactor design code such as MCNP. It is important to stress that TRIMON implements a method which is yet established by any other Monte Carlists, thus, thorough simulation validation and tests must be done before releasing it to the users.

4.10.1 RTP Approach to Criticality Benchmark

In this core benchmark problem, the number of fuel elements inserted into Malaysian Puspati TRIGA Reactor (RTP) core was incremented and the corresponding value of k_{eff} was measured. The measurement was made for each subsequent number of fuel rods until the reactor core reaches criticality. The core configuration at the moment of criticality is designated as Core-0 configuration. Fig. 4.7 shows the comparisons of the results obtained from measurements, MCNP, TRIGLAV and TRIMON.

In the simulation, the problem conditions were set so that they reproduce the conditions of the reactor core during the actual measurements. The temperature of the coolant was set at 293K, the reactor core was xenon-free, and the power of the reactor is at negligible thermal power (<0.01kW). In this experiment, all of the loaded fuels are of 8.5%wt fresh fuels (zero burnup level).

A total of 30000 neutron histories were simulated per fission cycle. The criticality calculation was done for 200 cycles with 30 skipped cycles. The number of cycles was chosen to ensure that the relative errors of the averaged tallies obtained using MCNP and TRIMON falls below 0.1%. It is important to note that (Brown, 2011) recommends using more than 10000 neutron histories for all simulations to avoid significant bias in k_{eff} and any local tallies in MCNP.

The plot of k_{eff} versus the number of fuel elements exhibit significant agreement between the simulation results with the experimental results at high fuel element count. The plot also exhibits strong agreement between TRIMON, MCNP and TRIGLAV. TRIMON predicts that the criticality is achieved after 66 fuel elements are inserted in the reactor core where the critical core k_{eff} is 1.00095 ± 0.00015. The validity of the simulation result is supported by the experimental plot where criticality was finally achieved after adding a similar number of fuel elements where the measured value of k_{eff} is 1.001.

The difference between the value of k_{eff} obtained from TRIMON and the actual experiment at the point of criticality is ~5 pcm. Since the systematic error of TRIMON is 0.00015 (~15 pcm), the predicted value of k_{eff} is well within the expected systematic error interval.

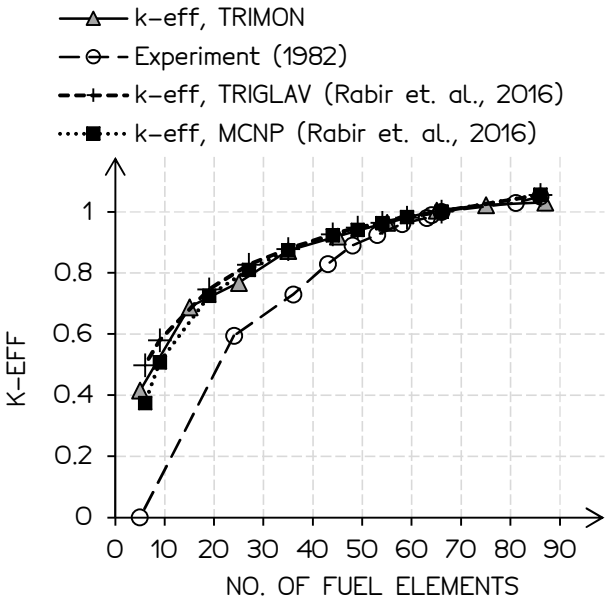

Figure 4.7: Approach to criticality curve.

Inevitably, there is a significant departure of the measured values of k_{eff} from simulated values of k_{eff} at lower fuel elements count. Specifically, this departure is caused by a smaller number of signals received by the detector as a result of its relatively large distance from the active core region. As the number of fuels increased,

the active core region is becoming bigger and closer to the detector which is located outside the reactor. As a result, the measurements' uncertainty was significantly reduced.

4.10.2 TRIMON k_{eff} Comparison with Measured RTP Operational Core Data

In the operational core benchmark problem, the mixed core configurations of RTP which consists of 8.5%wt and 12%wt UZrH fuel elements were considered. To assess the reliability of TRIMON, the results of the criticality calculations the first six operational core configurations were compared with the measured operational data obtained from the operational logbook of RTP. In these criticality calculations, 30000 neutron histories were used for each fission cycle and 200 fission cycles with 30 skipped cycles were performed using TRIMON. For additional information, the reactor normally operates six (6) hours per day for four days a week. The details of the operation histories of RTP for the first six operational cores are given in Table 4.2. The summary of the results of the comparison is given in Table 4.3.

Table 4.2: Histories of the first six RTP operational cores.

Core	Average Power (kW)	Total Burnup Given (MWd)	Accumulated Burnup (MWd)	Operating Hours (days)
Core-1 (C1)	455.015	43.4	43.4	95.3
Core-2 (C2)	600.580	45.8	89.2	76.4
Core-3 (C3)	674.223	42.6	131.8	63.1
Core-4 (C4)	727.700	87.1	218.9	119.7
Core-5 (C5)	706.565	19.6	238.5	27.8
Core-6 (C6)	736.874	78.0	316.5	105.8

Table 4.3: Summary of criticality calculations using TRIMON for Core-1 to Core-6. Measured k_{eff} obtained from the RTP operational logbook is also given. Difference between calculated and measured, Δk_{eff}, is also given.

Core	k_{eff} TRIMON	k_{eff} Measured	Δk_{eff}
Core-1 (C1) BOC	1.05190 ± 0.00028	1.05312 ± 0.00038	0.00122 ± 0.00047
Core-1 (C1) EOC	1.03310 ± 0.00030	1.03095 ± 0.00037	0.00215 ± 0.00048
Core-2 (C2) BOC	1.05701 ± 0.00043	1.05377 ± 0.00039	0.00324 ± 0.00058
Core-2 (C2) EOC	1.03702 ± 0.00038	1.04004 ± 0.00038	0.00298 ± 0.00054
Core-3 (C3) BOC	1.05432 ± 0.00026	1.05323 ± 0.00039	0.00109 ± 0.00047
Core-3 (C3) EOC	1.04258 ± 0.00039	1.04193 ± 0.00038	0.00065 ± 0.00055
Core-4 (C4) BOC	1.06005 ± 0.00044	1.05657 ± 0.00039	0.00343 ± 0.00059
Core-4 (C4) EOC	1.03624 ± 0.00043	1.03883 ± 0.00038	0.00259 ± 0.00057
Core-5 (C5) BOC	1.05102 ± 0.00049	1.05183 ± 0.00039	0.00081 ± 0.00063
Core-5 (C5) EOC	1.04499 ± 0.00046	1.04882 ± 0.00039	0.00368 ± 0.00060
Core-6 (C6) BOC	1.04506 ± 0.00043	1.04867 ± 0.00038	0.00361 ± 0.00057
Core-6 (C6) EOC	1.03978 ± 0.00048	1.03936 ± 0.00038	0.00042 ± 0.00061

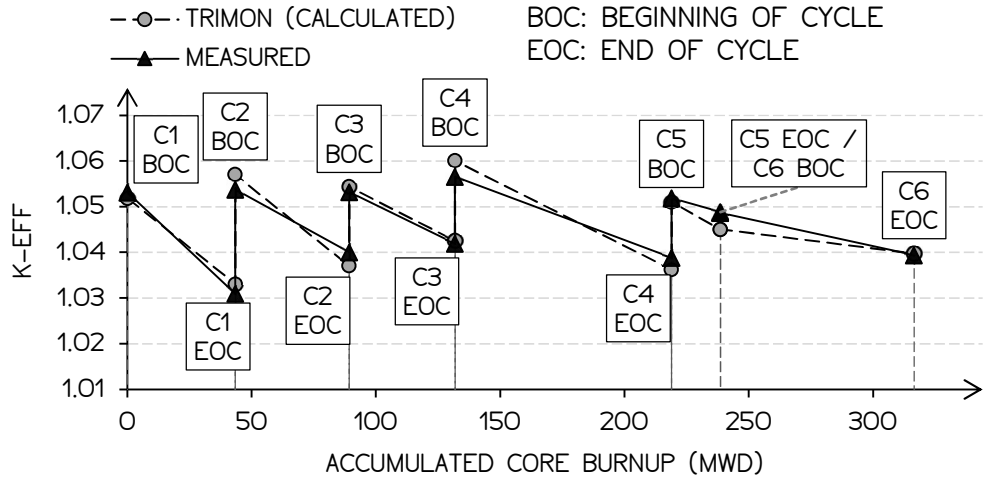

Figure 4.8: Core effective multiplication factors, k_{eff}, at zero core power versus accumulated core burnup in MWd from Core-1 to Core-6 (C1–C6).

The sawtooth-shaped plot depicted in Fig. 4.8 indicates a reduction of k_{eff} at the end of each operational core cycle (EOC) for both measured and calculated values. Then, the value of k_{eff} is restored every time the core is reconfigured at the beginning of cycle (BOC). During fuel reconfiguration, the existing high-burnup fuels may be replaced with new fresh fuels, or the same fuels loaded in the core may be reshuffled with the existing low-burnup fuels.

Each core configuration is assigned to a specific core identification, i.e. Core-N for the N^{th} operational core. When a specific core configuration has reached its end-of-cycle and reconfigured, the new core configuration is assigned to a new identification, i.e. Core-(N+1). It is important to note that the four control rods are assumed to be fully withdrawn. Essentially, the fuel follower control rod model is approximated to a standard 8.5%wt fuel model and the transient rod model is approximated to an empty aluminium tube model.

Here, the simulations of the operational cores using MCNP is not present in this section since incorporating fuel burnup effect in MCNP calculation can be cumbersome and time-consuming. However, the MCNP result of the critical core (Core-0) and the first two operational cores (Core-1 and Core-2) will be presented in the next section. Some work done by (Chiesa et al., 2016; Rabir et al., 2017) proposed extra treatment to the MCNP simulation model in order to account the fuel burnup effect. On the other hand, TRIMON offers instant core burnup consideration without the need for extra work on the simulation model. Fig. 4.9 shows the local fuel burnup calculation results produced by TRIMON.

For all simulated core configurations, the measured multiplication factors were compared with the result obtained using TRIMON. Interestingly, the average percentage difference of k_{eff} is less than 1% $\Delta k/k$, thus, indicating that TRIMON is a reliable tool to be used for core management analysis of RTP. For all configurations, the temperature of the coolant was set at 298K and the reactor was xenon-free. All fuel elements are of 8.5%wt and 20%wt, 19.9% enriched standard UZrH fuel.

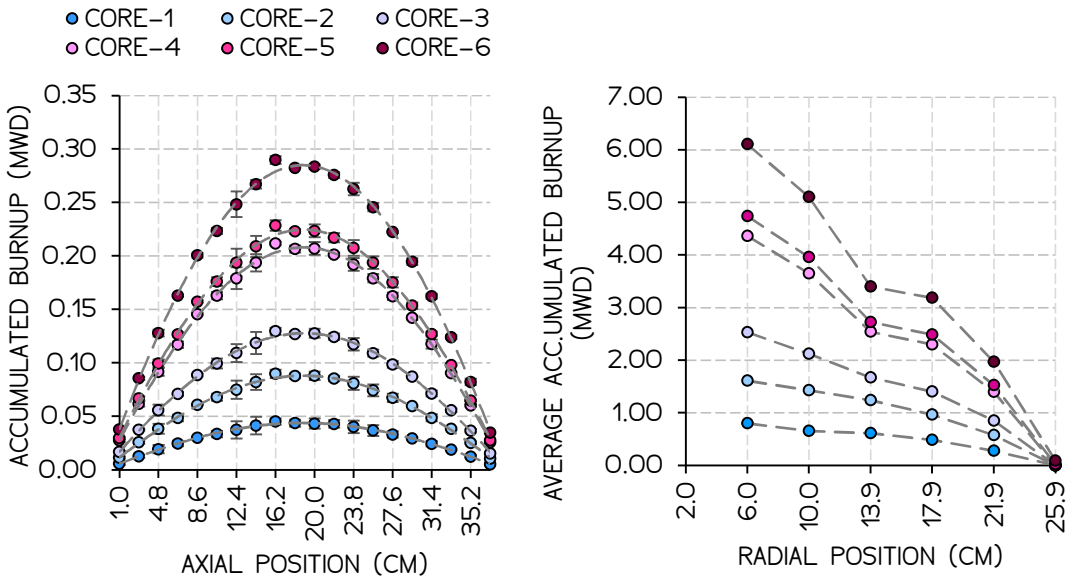

(a) (b)

Figure 4.9: (a) Locally accumulated burnup in MWd along the axial length of a standard 8.5%wt fuel calculated using TRIMON. The fuel remains loaded in the reactor core throughout the six operational core configurations (C1–C6). (b) Average accumulated burnup at different core radial positions.

4.10.3 Comparison of TRIMON with MCNP Benchmark of RTP

In this benchmark problem, the criticality calculations of RTP critical core (Core-0), first operational core (Core-1) and burned core (Core-2) were performed using TRIMON and MCNP. Various tally results obtained using TRIMON and MCNP were compared for each of the three cores. In these criticality calculations, the tally results include the effective multiplication factor, fission reaction rate, total reaction rate, total flux and thermal flux. In addition, the performance of both TRIMON and MCNP in terms of simulation time and fission source convergence were also compared.

Essentially, these comparisons were made to assess the ability of TRIMON to reproduce the simulation results obtained using MCNP. Plus, this section reports the evaluation of the gain brought by TRIMON compared to the local information lost due to the use of homogenized neutron cross section data. The core location map of RTP core is shown in Fig. 4.10. The configuration of Core-0, Core-1 and Core-2 is depicted in Fig. 4.11 respectively.

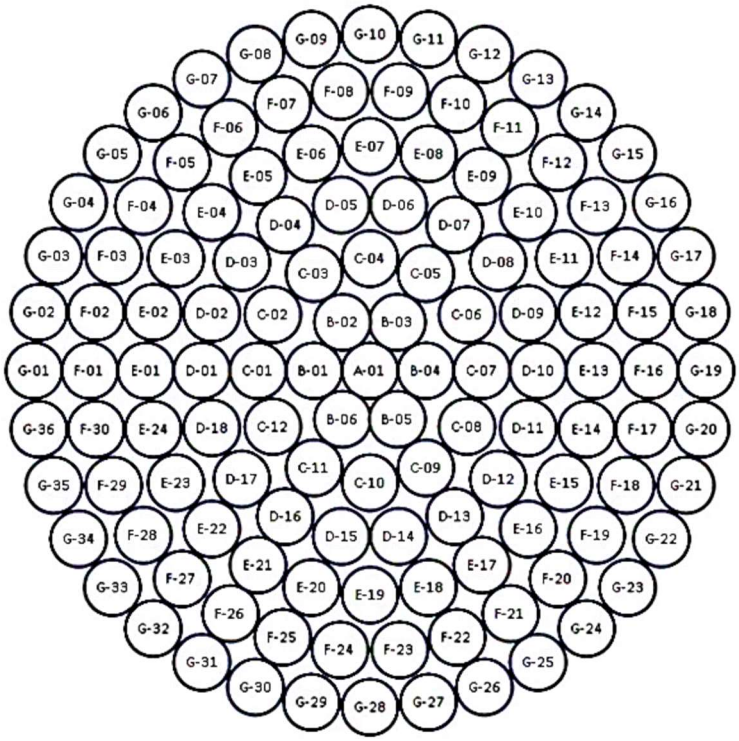

Figure 4.10: A 7-ring RTP core location identification map. A transient control rod (TROD) is located at C-04. Fuel follower control rods (FFCR) are located at D-01, D-10 and C-10.

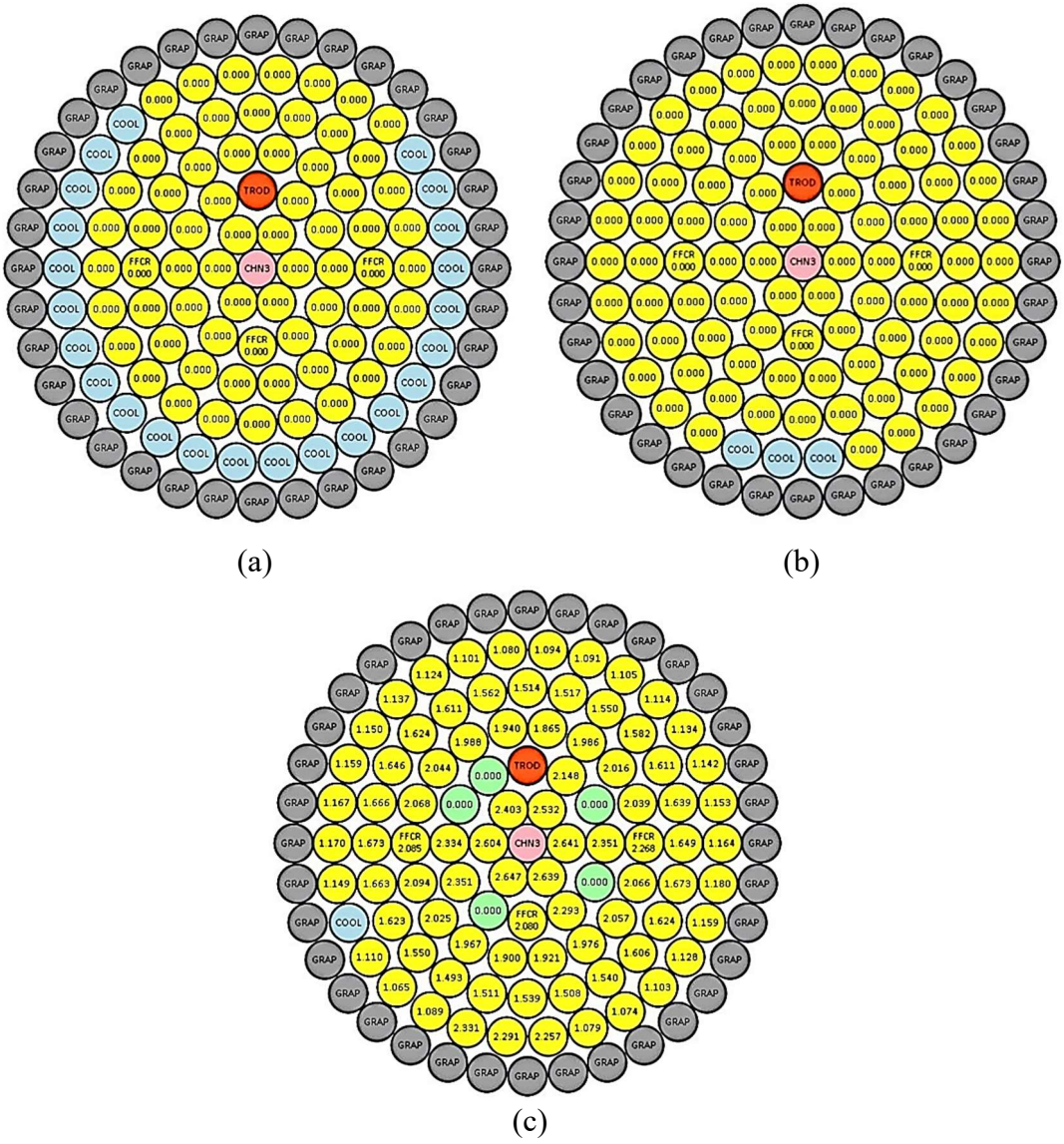

Figure 4.11: RTP operational core configurations (a) Critical core (Core-0) loaded with 66 fresh 8.5%wt UZrH fuels (yellow); (b) First operational core (Core-1) loaded with 86 fresh 8.5%wt UZrH fuels (yellow); (c) Second operational core (Core-2) loaded with 83 spent 8.5%wt UZrH fuels (yellow) and 5 fresh 12%wt UZrH fuels (green). Note: Numeric label indicates the fuel burnup in percent U-235.

Again, the control rods are assumed to be fully withdrawn, and this applies to all TRIMON and MCNP simulations of Core-0, Core-1 and Core-2. Here, all fuel follower control rods (FFCR) were replaced with standard 8.5%wt UZrH fuels, the transient control rod (TROD) was approximated using a void aluminium tube model and the central thimble of the reactor was replaced with a full water-filled aluminium tube model (CHN3).

Table 4.4 summarizes the effective multiplication factors, k_{eff}, and the total simulation time of the criticality calculations performed using TRIMON and MCNP for the three core configurations. For each criticality calculation, the number of neutron histories per cycle was increased to 50000 compared to the calculations done in the previous sections. This was done to further reduce tally bias in TRIMON and MCNP especially in mixed fuels and burned cores so that comparisons can be made at better accuracy. These calculations were performed using 200 fission cycles. The evolution of the relative error of k_{eff} obtained using TRIMON and MCNP over 170 active cycles for the three cores is shown in Fig. 4.12. It can be observed that TRIMON impose a slightly extra uncertainty due to the use of homogenized cross section data. However, these extra uncertainties are much smaller compared to the extra simulation time consumed by MCNP. Fig. 4.13 shows the plot of CPU wall clock in minutes versus fission cycle. Plots in Fig. 4.13 can be interpreted as the total time required to accomplish a certain number of fission cycles.

The number of skip cycles was set to 30 for both TRIMON and MCNP to ensure that the fission source distribution entropy completely converges with minimum standard deviation. Hence, active fission cycles begin at cycle 31 where tallies accumulation and k_{eff} averaging was started.

Table 4.4: Effective multiplication factors and total CPU time for completing 200 fission cycles, 50000 neutrons/cycle.

Core	$\boldsymbol{k_{\text{eff}}}$ **(TRIMON)**	$\boldsymbol{k_{\text{eff}}}$ **(MCNP)**	$\boldsymbol{\Delta k_{\text{eff}}}$	**CPU Time (MCNP)**	**CPU Time (TRIMON)**
Core-0	1.00388 ± 0.00046	1.00411 ± 0.00040	0.00023 ± 0.00061	45.6 mins	13.7 mins
Core-1	1.05154 ± 0.00046	1.05971 ± 0.00034	0.00817 ± 0.00057	40.4 mins	11.9 mins
Core-2	1.05752 ± 0.00042	1.05653 ± 0.00039	0.00099 ± 0.00057	273.6 mins	12.54 mins

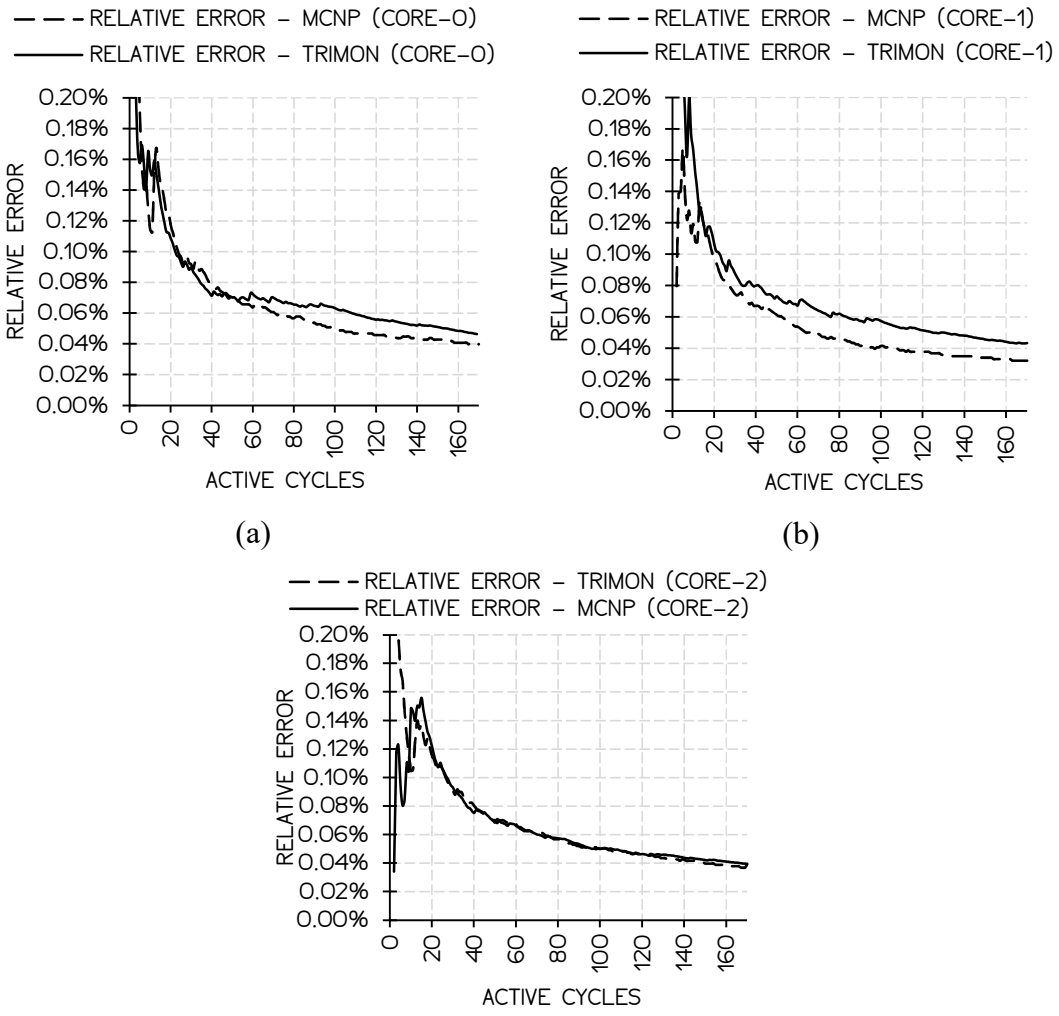

Figure 4.12: Relative error evolution for (a) Core-0, (b) Core-1 and (c) Core-2.

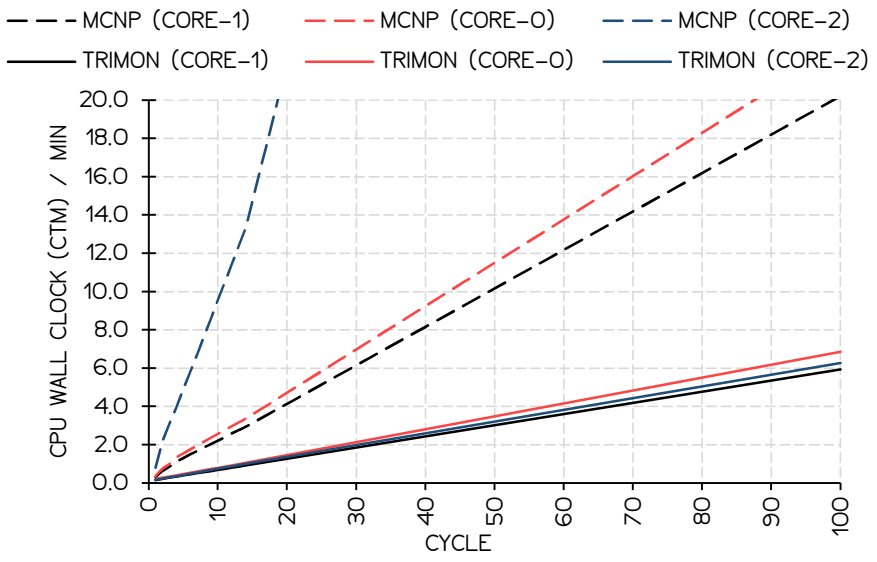

Figure 4.13: CPU wall clock of the first 100 cycles using TRIMON and MCNP.

In this benchmark problem, both TRIMON and MCNP codes were executed using the same machine. Both codes were also executed once at a time using Intel Core-i7 CPU @2.8GHz speed. It can be deduced that TRIMON has a better computational speed. Table 4.5 shows the figure of merit (FOM) of all reactor core calculations. Larger FOM is preferred because it means that less computational time is required to achieve a certain level of error, or in other words, the computation is more efficient.

Table 4.5: Figure of merit (FOM) of TRIMON and MCNP.

Core Configuration	**FOM = 1 / (CPU Time × Relative Error^2)**	
	TRIMON	**MCNP**
Core-0	411293	98075
Core-1	517744	154784
Core-2	600876	39878

Table 4.6: Convergence results for Core-0, Core-1 and Core-2 using TRIMON and MCNP.

	Core-0	**Core-1**	**Core-2**
Converged Cycle (TRIMON)	3	3	4
Converged Cycle (MCNP)	9	8	8
Converged Time (TRIMON)	20.0s	19.0s	25.1s
Converged Time (MCNP)	142.2s	112.2s	516.6s
Converged $\boldsymbol{H}_{\mathbf{src}}$ (TRIMON)	10.120 ± 0.001	10.480 ± 0.001	10.460 ± 0.001
Converged $\boldsymbol{H}_{\mathbf{src}}$ (MCNP)	8.640 ± 0.002	8.697 ± 0.001	9.350 ± 0.001

In the MCNP model of Core-0, Core-1 and Core-2, the reaction rates, total flux and thermal flux tallies were scored over the entire fuel rod cells plus the surrounding coolant water cell. Whereas in TRIMON, the tally volume of these quantities is integrated over all homogenized unit cells (as shown in Fig. 4.1) that build the entire fuel rod plus the surrounding coolant water. In TRIMON, scoring tallies over a region smaller than a unit cell is prohibited since TRIMON utilized spatially homogenized neutron cross section data. Thus, the same tally criteria are imposed to non-fuel cells such as coolant cell, graphite element cell etc.

The accumulated tallies obtained using TRIMON and MCNP were then normalized to a total of one reaction for reaction rates, a total of one neutron for the total flux and a total of one thermal neutron for the thermal flux. The normalization of these quantities was done to make the comparison simple and perceivable. The plot of the total flux, thermal flux, total reaction rate, and fission rate for Core-0, Core-1 and

Core-2 are shown in Figs. 14.14-14.16 respectively. The relative differences in per cent of these quantities are also shown in these figures.

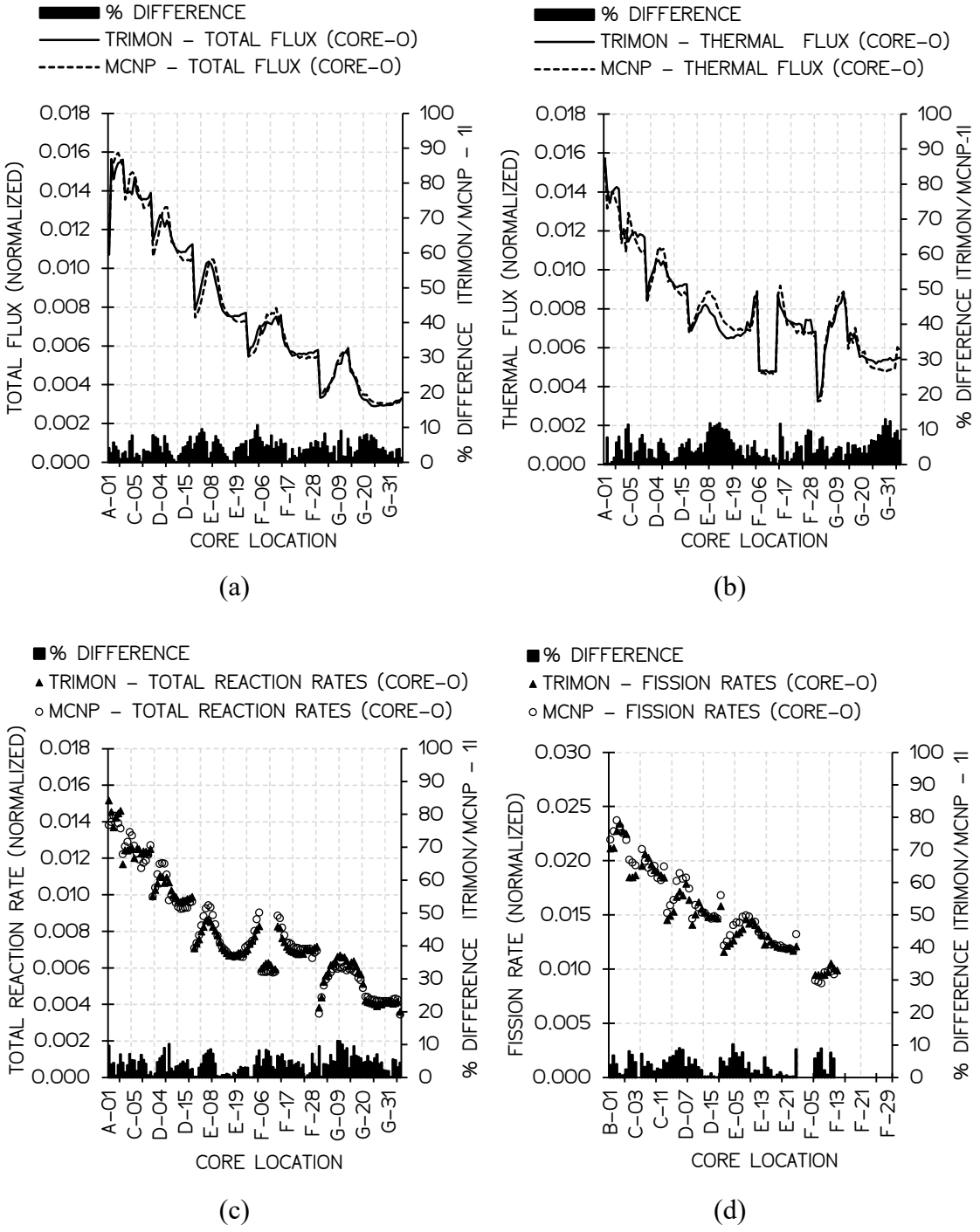

Figure 4.14: The plots of (a) total flux, (b) thermal flux, (c) total reaction rate and (d) fission rates across the entire core locations of Core-0. Note: The fluxes and the reaction rates are normalised to one neutron and one reaction respectively.

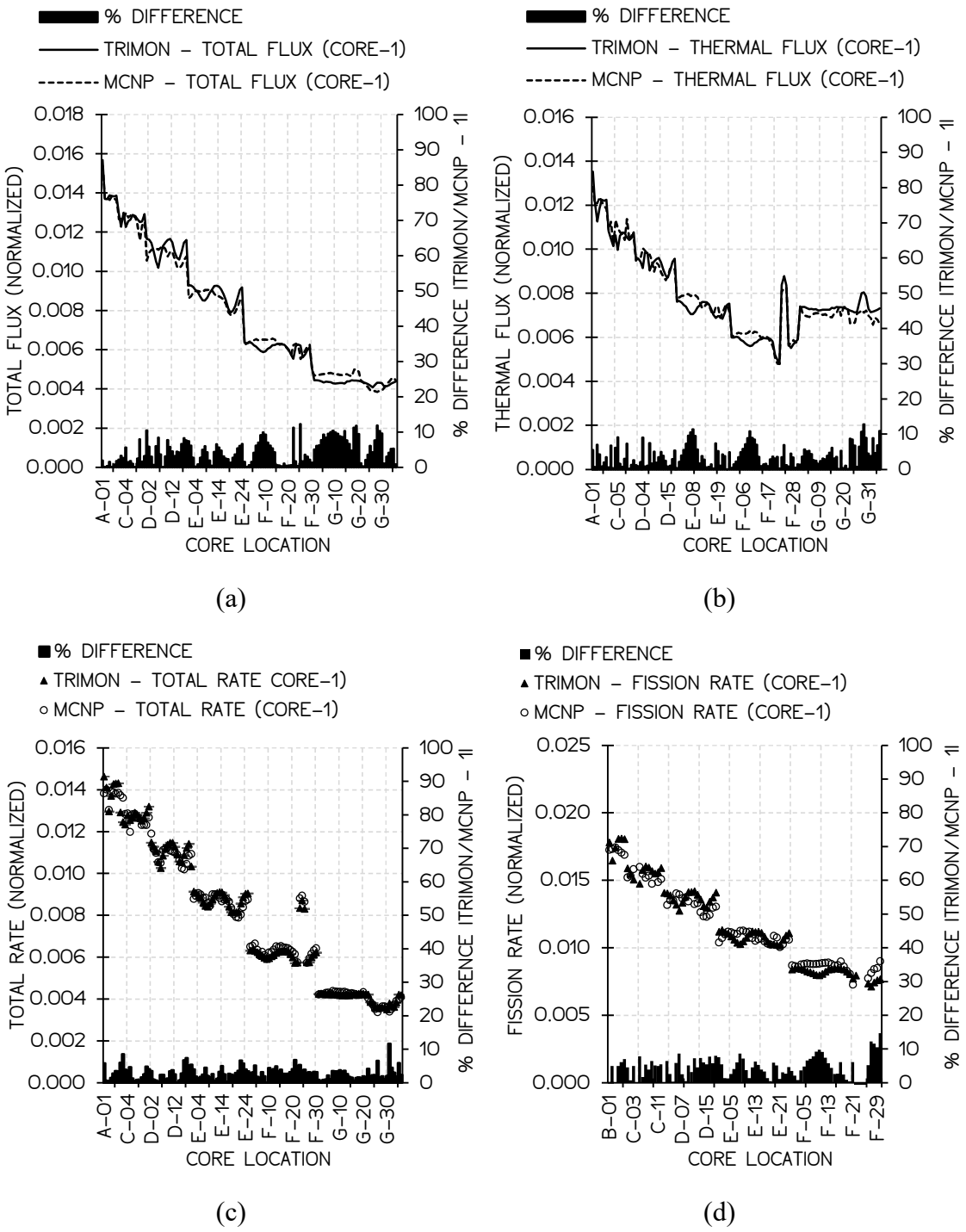

Figure 4.15: The plots of (a) total flux, (b) thermal flux, (c) total reaction rate and (d) fission rates across the entire core locations of Core-1. Note: The fluxes and the reaction rates are normalised to one neutron and one reaction respectively.

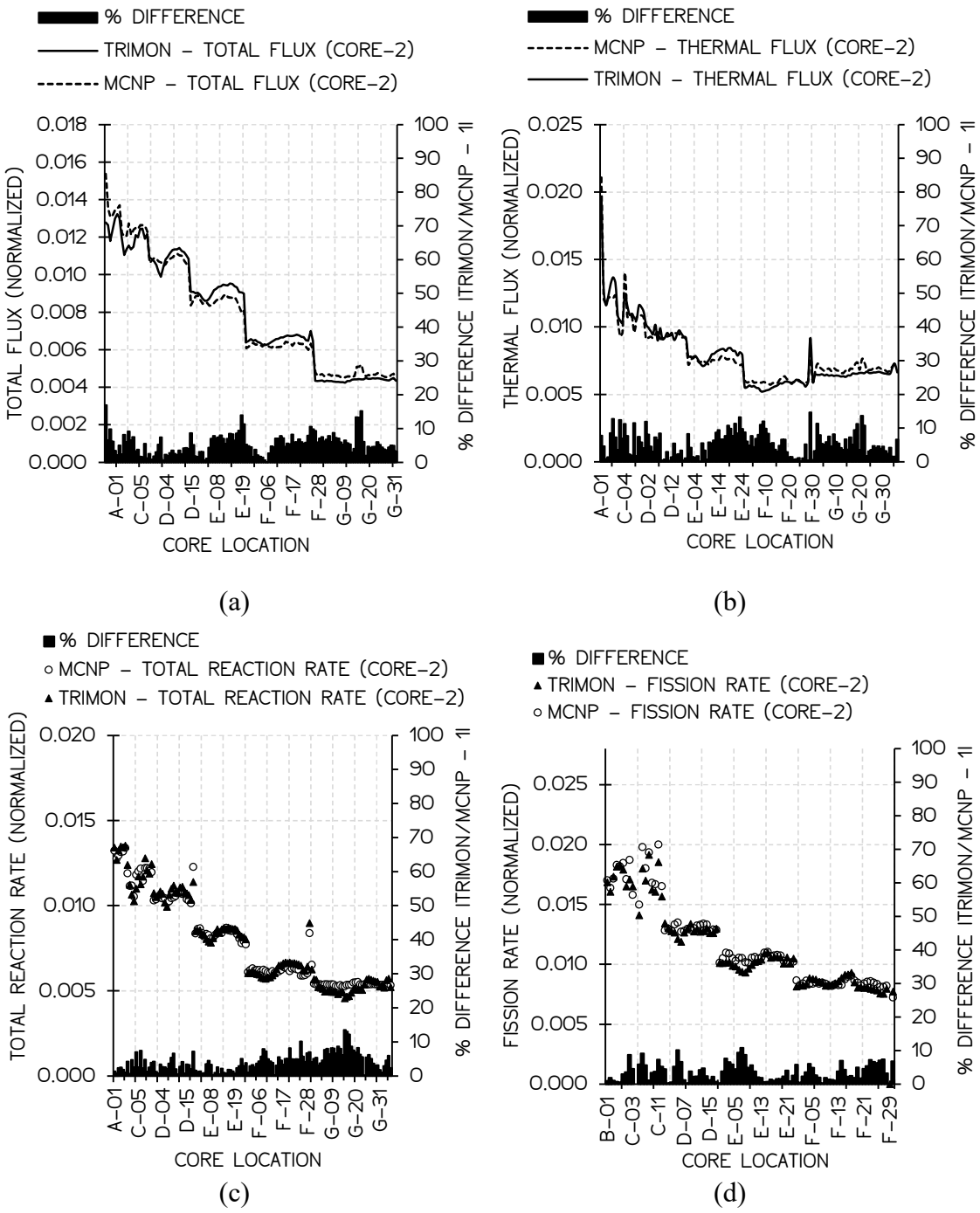

Figure 4.16: The plots of (a) total flux, (b) thermal flux, (c) total reaction rate and (d) fission rates across the entire core locations of Core-2. Note: The fluxes and the reaction rates are normalised to one neutron and one reaction respectively.

4.11 Discussions

Aside from demonstrating the feasibility of using homogenized cross section data in the Monte Carlo method, TRIMON also intends to offer robust core calculations to the end-users. As a result, TRIMON permits users to operate calculations with the consideration of local core burnups.

Fundamentally, the first step to integrating homogenized group data in the Monte Carlo method is simply to reduce the complexity of the stochastic simulation. On the other hand, simulating neutron transport processes in an actual reactor using a point-wise energy cross section data require a detailed reactor core model which requires more computational time. In most instances, a detailed core model is not necessary because the reflection of the entire core behaviour is more significant.

Authors in (Rabir et al., 2016) demonstrated that thousands of MCNP criticality calculation cycles were required to converge at a good estimation of k_{eff} values. The work done by (Wang et al., 2015) also emphasized on speeding up the convergence of source distribution and k_{eff} due to the similar slow convergence problem. Notably, TRIMON addressed this issue by introducing the homogenized cross section in the Monte Carlo method to reduce the spatial variation of neutron cross sections within the reactor core. Hence, it indirectly coarsens the spatial variation of the source distribution, thus relaxing the complexity of the source converging process. However, this attempt sacrifices the tally resolution where the highest resolution is only up to a unit cell level.

Conventional point-wise energy Monte Carlo method requires spatially dependent neutron cross section data, where the detail of cross section variations across the unit cell volume must be known. However, the case is different for homogenized unit cells. Recall that a homogenized unit cell is the spatial average of a heterogeneous unit cell, V, containing various material regions of different neutron cross sections. In this perspective, the volume integrated flux and the net reaction rate in V are the same in both heterogeneous unit cell and its equivalent homogeneous unit cell. As a result, the true k_{eff} value of both heterogeneous and homogeneous unit cells is preserved.

In fact, all sequences of collision events that occur within a heterogeneous unit cell volume are not statistically identical with the collision events that occur within the equivalent homogeneous unit cell volume. Moreover, all collision events within a homogeneous unit cell volume are virtual, however, these virtual collisions preserve the total neutron energy deposited inside the entire geometry of the unit cell. Plus, the integral of the neutron track lengths between these virtual collision events that occur within the entire unit cell volume is also preserved. Due to the implication of these virtual events, tallies should be strictly scored over the entire volume of the unit cell and scoring should not be done in the smaller sub-region of the unit cell. Fortunately, the neutron behaviour over the entire cell is of much greater importance, thus the implication of the virtual collision events is negligible.

References

A. Persic, Slavic, S., Ravnik, M., & Zagar, T. (1998). *TRIGLAV - A Program Package for Research Reactor Calculations*.

Brown, F. B. (2011). "K-effective of the World" and Other Concerns for Monte Carlo Eigenvalue Calculations. *Progress in Nuclear Science and Technology*. https://doi.org/10.15669/pnst.2.738

Carter, L. L., & Cashwell, E. D. (1975). *Particle-transport simulation with the Monte Carlo method*. *Other Information: Orig. Receipt Date: 30-JUN-76*. https://doi.org/10.2172/4167844

Chiesa, D., Clemenza, M., Pozzi, S., Previtali, E., Sisti, M., Alloni, D., … Sartori, A. (2016). Fuel burnup analysis of the TRIGA Mark II reactor at the University of Pavia. *Annals of Nuclear Energy*, *96*, 270–276. https://doi.org/10.1016/j.anucene.2016.06.008

Cho, N. Z., & Chang, J. (2009). Some outstanding problems in neutron transport computation. *Nuclear Engineering and Technology*, *41*(4), 381–390. https://doi.org/10.5516/NET.2009.41.4.381

Duderstadt, J. J., & Hamilton, L. J. (1976). Nuclear Reactor Analysis. *Mechanical Engineering*. https://doi.org/10.1109/TNS.1977.4329257

Henry, R., Tiselj, I., & Snoj, L. (2017). CFD/Monte-Carlo neutron transport coupling scheme, application to TRIGA reactor. *Annals of Nuclear Energy*, *110*, 36–47. https://doi.org/10.1016/J.ANUCENE.2017.06.018

International Atomic Energy Agency (IAEA). (1980). A new approach to homogenization and group condensation. *Specialists' Meeting on Homogenization Methods in Reactor Physics*, *231*(November 1978), 303–322.

Leppänen, J. (2010). Performance of Woodcock delta-tracking in lattice physics applications using the Serpent Monte Carlo reactor physics burnup calculation code. *Annals of Nuclear Energy*, *37*(5), 715–722. https://doi.org/10.1016/J.ANUCENE.2010.01.011

Peršič, A., Žagar, T., Ravnik, M., Slavič, S., Žefran, B., Ćalić, D., … Snoj, L. (2017). TRIGLAV: A program package for TRIGA reactor calculations. *Nuclear Engineering and Design*, *318*, 24–34. https://doi.org/10.1016/J.NUCENGDES.2017.04.010

Rabir, M. H. B., Mohamed Zin, M. R. B., Karim, J. B. A., Jalal Bayar, A. M. B., Usang, M. D. A., Mustafa, M. K. B., … Jalil, M. H. B. (2017). Neutronics calculation of RTP core. In *AIP Conference Proceedings* (Vol. 1799). https://doi.org/10.1063/1.4972907

Rabir, M. H., Md Zin, M. R., & Usang, M. D. (2016). Neutron flux and power in RTP core-15. *AIP Conference Proceedings*, *1704*(1), 50018. https://doi.org/10.1063/1.4940114

Romano, P. K., & Forget, B. (2013). The OpenMC Monte Carlo particle transport code. *Annals of Nuclear Energy*, *51*, 274–281. https://doi.org/10.1016/j.anucene.2012.06.040

Ross, S., & Ross, S. (2013). Generating Discrete Random Variables. *Simulation*, 47–68. https://doi.org/10.1016/B978-0-12-415825-2.00004-8

Snoj, L., & Ravnik, M. (2008). Power peakings in mixed TRIGA cores. *Nuclear Engineering and Design*, *238*(9), 2473–2479. https://doi.org/10.1016/j.nucengdes.2008.02.005

Trkov, A., & Ravnik, M. (1994). Effective diffusion homogenization of cross sections for pressurized water reactor core calculations. *Nuclear Science and Engineering*, *116*(2), 86–95. Retrieved from http://www.scopus.com/inward/record.url?eid=2-s2.0-0028377664&partnerID=tZOtx3y1

Wang, K., Li, Z., She, D., Liang, J., Xu, Q., Qiu, Y., … Yu, G. (2015). RMC - A Monte Carlo code for reactor core analysis. *Annals of Nuclear Energy*, *82*, 121–129. https://doi.org/10.1016/j.anucene.2014.08.048

X-5 Monte Carlo Team. (2005). MCNP - A General Monte Carlo N-Particle Transport Code, Version 5. *Los Alamos Nuclear Laboratory*, *I*, 2-71-2–80. https://doi.org/LA-UR-03-1987